

*Structural and Molecular Diversification
of the Anguimorpha Lizard Mandibular
Venom Gland System in the Arboreal
Species Abronia graminea*

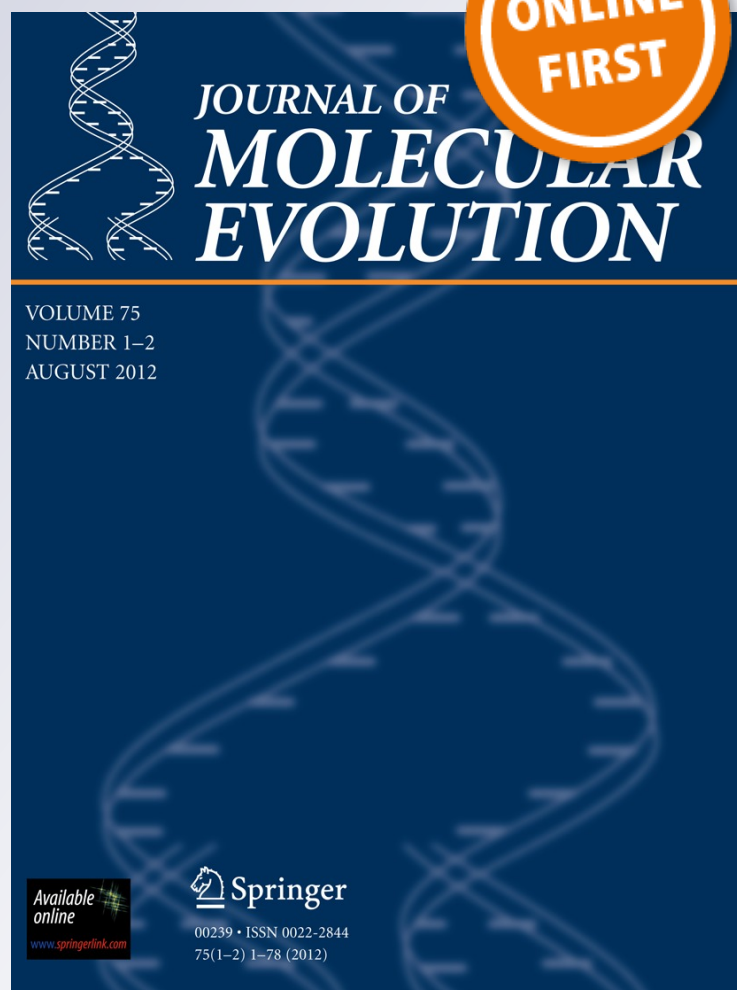
**Ivan Koludarov, Kartik Sunagar,
Eivind A. B. Undheim, Timothy
N. W. Jackson, Tim Ruder, Darryl
Whitehead, Alejandro C. Saucedo et al.**

Journal of Molecular Evolution

ISSN 0022-2844

J Mol Evol

DOI 10.1007/s00239-012-9529-9



Your article is protected by copyright and all rights are held exclusively by Springer Science +Business Media New York. This e-offprint is for personal use only and shall not be self-archived in electronic repositories. If you wish to self-archive your work, please use the accepted author's version for posting to your own website or your institution's repository. You may further deposit the accepted author's version on a funder's repository at a funder's request, provided it is not made publicly available until 12 months after publication.

Structural and Molecular Diversification of the Anguimorpha Lizard Mandibular Venom Gland System in the Arboreal Species *Abronia graminea*

Ivan Koludarov · Kartik Sunagar · Eivind A. B. Undheim · Timothy N. W. Jackson · Tim Ruder · Darryl Whitehead · Alejandro C. Saucedo · G. Roberto Mora · Alejandro C. Alagon · Glenn King · Agostinho Antunes · Bryan G. Fry

Received: 15 May 2012 / Accepted: 29 October 2012
© Springer Science+Business Media New York 2012

Abstract In the past, toxinological research on reptiles has focused principally on clinically important species. As a result, our understanding of the evolution of the reptile venom system is limited. Here, for the first time, we describe the structural and molecular evolutionary features of the mandibular toxin-secreting gland of *Abronia graminea*, a representative of one of the poorly known and entirely arboreal lineages of anguimorph lizards. We show that the mandibular gland is robust and serous, characters

consistent with those expected of a toxin-secreting gland in active use. A wide array of transcripts were recovered that were homologous to those encoded by the indisputably venomous helodermatid lizards. We show that some of these toxin transcripts are evolving under active selection and show evidence of rapid diversification. Helokinestatin peptides in particular are revealed to have accumulated residues that have undergone episodic diversifying selections. Conversely, the natriuretic peptides have evolved under tremendous evolutionary constraints despite being encoded in tandem with helokinestatins by the same gene precursor. Of particular note is the sequencing for the first time of kunitz peptides from a lizard toxin-secreting gland. Not only are kunitz peptides shown to be an ancestral toxicoferan toxin, the ancestral state of this peptide is revealed to be a dual domain encoding precursor. This research provides insight into the evolutionary history of the ancient toxicoferan reptile venom system. In addition, it shows that even ‘clinically irrelevant’ species can be a rich source of novel venom components, worthy of investigation for drug design and biomedical research.

Ivan Koludarov, Kartik Sunagar and Eivind A. B. Undheim are Co-first authors.

I. Koludarov · E. A. B. Undheim · T. N. W. Jackson · T. Ruder · B. G. Fry (✉)
Venom Evolution Laboratory, School of Biological Sciences, University of Queensland, St. Lucia, QLD 4072, Australia
e-mail: bgfry@uq.edu.au

E. A. B. Undheim · G. King
Institute for Molecular Biosciences, University of Queensland, St. Lucia, QLD 4072, Australia

K. Sunagar · A. Antunes
CIMAR/CIIMAR, Centro Interdisciplinar de Investigação Marinha e Ambiental, Universidade do Porto, Rua dos Bragas, 177, 4050-123 Porto, Portugal

K. Sunagar · A. Antunes
Departamento de Biologia, Faculdade de Ciências, Universidade do Porto, Rua do Campo Alegre, 4169-007 Porto, Portugal

D. Whitehead
School of Biomedical Sciences, University of Queensland, St. Lucia, QLD 4072, Australia

A. C. Saucedo · G. R. Mora · A. C. Alagon
Departamento de Medicina Molecular y Bioprocesos, Instituto de Biotecnología, Universidad Nacional Autónoma de México, Av. Universidad 2001, 62210 Cuernavaca, Morelos, Mexico

Keywords Venom · Phylogeny · Molecular evolution

Introduction

The evolution of reptilian venoms has previously been inferred to have occurred at the base of a strongly supported clade termed the Toxicofera (Anguimorpha, Iguania and Serpentes) (Fry et al. 2006; Vidal and Hedges 2005; Wiens et al. 2012). Whilst nuclear gene sampling has been unable to resolve the relative relationships within this clade, the use of SINES has been useful (Piskurek et al. 2006). Critical to this conclusion of a single early evolution

of reptile venom was evidence that toxin genes sampled from a variety of toxicofera taxa demonstrated monophyly of lizard and snake toxins to the exclusion of non-venom homologues and that in some cases snake and lizard genes were not reciprocally monophyletic (Fry et al. 2006, 2010a). One limitation to this approach is the potential influence incomplete sampling of gene homologues (i.e. both venom and non-venom duplicate genes) could have upon phylogenetic analyses—potentially resulting in gene trees that falsely depict toxin genes as monophyletic (cf. Casewell et al. 2012). However, the incorporation of recently sampled non-venom gene homologues into toxin family gene trees provided further support for the single early origin hypothesis, with character reconstruction analyses supporting the premise that reptile venom evolved at the base of the Toxicofera (Casewell et al. 2012).

Historically, the two members of the genus *Heloderma* were considered the only venomous lizards. However, recent discoveries on the origins of venom and associated structures in snakes and lizards have however, led to a paradigm shift in our understanding of the evolution of squamate venom systems (Vidal and Hedges 2005; Fry et al. 2006, 2009a, b, 2010a, b, 2012). The current data suggest that venom in reptiles appeared approximately 170 million years ago and that all modern venomous reptiles share a common venomous ancestor. As a result, these animals have been collectively placed in the clade Toxicofera. The ancestral toxicofera reptile possessed both maxillary and mandibular serous dental glands of relatively simple structure. These glands produced pharmacologically active compounds that acted as a substrate for the subsequent evolution of all the reptilian toxins. Iguanian lizards diverged whilst this system was still in a primitive state, and thus their dental glands apparently conferred no ecological advantage and have either been secondarily lost completely or retained in a seemingly incipient condition. The remainder of the clade subsequently split into two major radiations: the snakes, which evolved complex maxillary glands and in many cases lost the mandibular glands entirely and the anguimorph lizards in which the mandibular glands were retained and diversified whilst the maxillary glands were lost completely in all but one species examined to-date.

As the toxin-secreting systems of anguimorph lizards have received less attention than those of the more medically important venomous snakes, it remains unknown to what extent different toxin types have undergone structural and functional innovation within this major clade. Detailed knowledge of the Anguimorpha toxins is crucial for understanding of the structure, function and composition of the ancestral Toxicofera venom system, as well as for investigation of the parallel diversification of the venom system in the two primary clades of venomous reptiles.

Helodermatid lizards produce clinically complex envenomations with symptoms including extreme pain, acute local swelling, nausea, fever, faintness, myocardial infarction, tachycardia, hypotension and inhibition of blood coagulation (Bogert and del Campo 1956; Bouabboud and Kardassakis 1988; Hooker and Caravati 1994; Strimple et al. 1997; Cantrell 2003; Beck 2005). Venom studies have revealed a great diversity of components present in the venom of helodermatid lizards (Table 1). Previous work by us has shown that all anguimorph lizards share a core toxin arsenal produced by the mandibular toxin-secreting gland (Table 1; (Fry et al. 2006, 2009b, 2010b)).

In our studies to-date, we have shown that Anguimorpha mandibular gland transcripts indeed encode bioactive peptides and proteins, with targets ranging from anti-platelet (type III phospholipase A₂) to novel peptides acting upon the cardiovascular system (celestoxin, cholecystokinin, goanatyrotoxin, helokinestatin and natriuretic) (Fry et al. 2006, 2009a, b, 2010a, b). Despite even non-helodermatid anguimorph species being a rich source of novel compounds, within the family Anguinae only three species have previously had their venom systems studied: *Gerrhonotus infernalis* (terrestrial), *Celestus warreni* (semi-fossorial) and *Pseudopus apodus* (fossorial) (Fry et al. 2010b). In particular, arboreal lineages have not been studied to-date. We address this imbalance by conducting in-depth analyses of the transcripts from the mandibular toxin-secreting gland of *Abronia graminea*, an arboreal generalist predator of both invertebrates and small vertebrates such as skinks. The results provided insights into toxin evolutionary history and the selection pressures that might have shaped them. Of particular focus were the natriuretic and helokinestatin peptides, which uniquely share a precursor, with the helokinestatins being a de novo evolution within the natriuretic precursor.

Materials and Methods

Species Examined

Four *A. graminea* specimens were field collected by BGF and ACS from Esperance, Mexico under the University of Melbourne Animal Ethics approval number 03126. Animals were placed under surgical level anesthesia using Zoletil and euthanized by decapitation whilst under anesthesia. Glands were then dissected or heads preserved in formalin.

Histology

Histological sections were prepared from one specimen. Whole heads were removed and a cut was made to the

Table 1 Anguimorpha lizard toxin mRNAs sequences recovered in this study

Toxin type	Bioactivity
Celestotoxin	Hypotensive (Fry et al. 2010a)
Cholecystokinin	Hypotensive through blockage cholecystokinin receptor-A (Fry et al. 2010a)
CRiSP	Blockage of ryanodine receptors, and potassium channels producing lethargy, paralysis and hypothermia (Mochcamorales et al. 1990; Morrisette et al. 1994, 1995; Nobile et al. 1994, 1996)
Exendin	Cardiotoxic (Fry et al. 2010b)
Goannatyrotoxin	Hypertensive/hypotensive triphasic effect (Fry et al. 2010a)
Helokinstatin	Bradykinin inhibition (Fry et al. 2010a, b; Kwok et al. 2008; Ma et al. 2012)
Helofensin	Neurotoxin that inhibits direct electrical stimulation (Komori et al. 1988).
Hyaluronidase	Venom spreading factor (Tu and Hendon 1983)
Kallikrein	Release of bradykinin from kinogen (Mebs 1969a, b; Nikai et al. 1988, 1992; Utaisincharoen et al. 1993). A derivative form also known to cleave fibrinogen (Datta and Tu 1997).
Lectin	Uncharacterised in lizard venoms; snake venom forms have been shown to have various modes of action upon platelet aggregation (Clemetson et al. 2005; Morita 2005).
Natriuretic peptide	Hypotension induction leading to loss of consciousness; mediated through the binding of GC-A resulting in the relaxation of cardiac smooth muscle (Fry et al. 2005, 2006, 2009b, 2010a, b).
Nerve growth factor	Uncharacterised
PLA ₂	Inhibition of epinephrine-induced platelet aggregation (Fry et al. 2006; Huang and Chiang 1994).
Scaffolds known only from transcripts and with bioactivities still to be characterised	
Epididymal secretory protein	(Fry et al. 2010a)
Ribonuclease	(Fry et al. 2010a)

underside to allow fast penetration of the fixative (10 % neutral buffered formalin). After a minimum of 2 days excess tissue was removed and the head immersed in Kristensen's decalcification solution and placed on a rotor for 3 weeks. Before processing the head was bisected longitudinally for cutting transversely, at three microns, in two separate blocks. The processing schedule was: 10 % Formalin 2 h; Absolute ethanol 4 × 1 h; Histolene 3 × 1 h; Paraffin wax 2 × 90 min. The sections were taken every 100 microns stained Masson's Trichrome stain.

cDNA Library Construction and Analysis

Mandibular toxin-secreting glands of three specimens were pooled and total RNA extracted using the standard TRIzol Plus method (Invitrogen). Extracts were enriched for mRNA using standard RNeasy mRNA mini kit (Qiagen) protocol. mRNA was reverse transcribed, fragmented and ligated to a unique 10-base multiplex identifier (MID) tag prepared using standard protocols and applied to one PicoTiterPlate for simultaneous amplification and sequencing on a Roche 454 GS FLX+ Titanium platform (Australian Genome Research Facility). Automated grouping and analysis of sample-specific MID reads informatically separated *A. graminea* sequences from the other transcriptomes on the plates, which were then post-processed to remove low quality sequences before de novo assembly using the MIRA software programme. Assembled contigs were processed using CLC Main Work Bench (CLC-Bio) and a variety of other bioinformatic tools to provide Gene Ontology, BLAST and domain/Interpro annotation (Conesa et al. 2005; Conesa and Gotz 2008; Gotz et al. 2008, 2011). The above analyses assisted in the rationalisation of the large numbers of assembled contigs into phylogenetic 'groups' for detailed phylogenetic analyses outlined below.

Phylogenetic Analyses

Phylogenetic analyses were performed to allow reconstruction of the molecular evolutionary history of each toxin type for which transcripts were bioinformatically recovered. Toxin sequences were identified by comparison of the translated DNA sequences with previously characterised toxins using BLAST search (Altschul et al. 1997) of the Swiss-Prot/Uni-Prot protein database (<http://www.expasy.org/tools/blast/>). Molecular phylogenetic analyses of toxin transcripts were conducted using the translated amino-acid sequences. Comparative sequences from other venomous reptiles and physiological gene homologues identified from non-venom gland transcriptomes were included in each dataset as outgroup sequences. To minimize confusion, all sequences obtained in this study are referred to by their Genbank accession numbers (<http://www.ncbi.nlm.nih.gov/sites/entrez?db=Nucleotide>) and sequences from previous studies are referred to by their UniProt/Swiss-Prot accession numbers (<http://www.expasy.org/cgi-bin/sprot-search-ful>). Resultant sequence sets were aligned using the programme CLC Mainbench. When presented as sequence alignments, the leader sequence is shown in lowercase and cysteines are highlighted in black. > and < indicate incomplete N/5' or C/3' ends, respectively. Datasets were analysed using Bayesian inference implemented on MrBayes, version 3.0b4 (Ronquist and Huelsenbeck 2003). The analysis was performed by running a minimum of 1 × 10⁷ generations in

four chains, and saving every 100th tree. The log-likelihood score of each saved tree was plotted against the number of generations to establish the point at which the log-likelihood scores of the analysis reached their asymptote, and the posterior probabilities for clades established by constructing a majority rule consensus tree for all trees generated after the completion of the burn-in phase.

Selection Analyses

In order to test whether natriuretic peptides and helokinestatsins were influenced by positive- or negative-selection pressures, we employed the maximum likelihood models of coding-sequence evolution implemented in CODEML in PAML (Yang 2007) programme package version 4, which compares the maximum likelihood estimates of dN and dS across an alignment to a predefined distribution and uses empirical Bayes methods to identify individual positively selected site (Nielsen and Yang 1998).

Site-specific models (Nielsen and Yang 1998) were employed for detecting diversifying selection across the sites in the helokinestatin and the natriuretic propeptide alignments. They statistically detect diversifying selection as a non-synonymous-to-synonymous nucleotide substitution rate ratio (ω) significantly greater than 1. Since no priori expectation exists for the distribution of ω values, we compared likelihood values for three pairs of models with different assumed ω distributions: M0 (constant ω rates across all sites) versus M3 (allows the ω to vary across sites within 'n' discrete categories, $n \geq 3$); M1a (a model of neutral evolution) where all sites are assumed to be either under negative ($\omega < 1$) or neutral selection ($\omega = 1$) versus M2a (a model of positive selection) which in addition to the site classes mentioned for M1a, assumes a third category of sites; sites with $\omega > 1$ (positive selection) and M7 (Beta) versus M8 (Beta and ω), and models that mirror the evolutionary constraints of M1 and M2 but assume that ω values are drawn from a beta distribution (Nielsen and Yang 1998). The estimations are considered significant, only if the alternative models (M3, M2a and M8: allow sites with $\omega > 1$) show a better fit in Likelihood-Ratio Test (LRT) relative to their null models (M0, M1a and M8: do not show allow sites $\omega > 1$). LRT is estimated as twice the difference in maximum likelihood values between nested models and compared with the χ^2 distribution with the appropriate degree of freedom (the difference in the number of parameters between the two models). The Bayes empirical Bayes (BEB) approach (Yang et al. 2005) was used to identify amino acids under positive selection by calculating the posterior probabilities that a particular amino acid belongs to a given selection class (neutral, conserved or highly variable). Sites with

greater posterior probability (PP $\geq 95\%$) of belonging to the ' $\omega > 1$ ' were inferred to be positively selected.

We further employed a lineage-specific two-ratio model as well as the optimized branch-site test (Yang and Nielsen 2002; Zhang et al. 2005) to assess selection pressures acting upon individual lineages. A LRT was conducted by comparing the two-ratio model that allows omega to be greater than 1 in the foreground branch, with the null model that does not. The branch-site model by comparison, allows omega to vary both across sites of the protein and across branches in the tree and has reasonable power and accuracy to detect short bursts of episodic adaptations (Zhang et al. 2005).

Detection of positive selection using the aforementioned lineage-specific methods requires the foreground (lineage to be tested for positive selection) and background branches (rest of the lineages) to be defined a priori. We used GA-Branch test (Pond and Frost 2005b) implemented in the HyPhy (Pond et al. 2005c) package that does not require this information and works on the principle that there could be many models that better fit the data than a single priori hypothesis and uses a robust multi-model inference to collate results from all models examined and provides confidence intervals on dN/dS for each branch. We also used the branch-site Random-effects likelihood (REL) (Pond et al. 2011) that performs a series of LRTs to identify lineages in the phylogeny that have a proportion of sites evolving under episodic diversifying selection pressures. The more advanced Mixed Effects Model Evolution (MEME) (Pond et al. 2011) was also used to detect episodic diversifying selection. MEME employs Fixed-effects likelihood (FEL) along the sites and REL across the branches to detect episodic diversifying selection. We employed REL, FEL and Single Likelihood Ancestor Counting (SLAC) models (Pond and Frost 2005a) to further provide significant support to the above analyses and to detect sites under positive and negative selection. For clear depiction of the proportion of sites under selection, an evolutionary fingerprint analysis was carried out using the ESD algorithm (Pond et al. 2011) implemented in Datamonkey.

It has been suggested that the maximum-likelihood method of evaluating positive-selection produces false-positive results when no positively selected sites exist (Suzuki and Nei 2004) or when positively and negatively selected sites are mixed (Anisimova et al. 2002). For this reason, further support for the PAML results was sought using a complementary protein level approach implemented in TreeSAAP (Woolley et al. 2003) which measures the selective influences on 31 structural and biochemical amino-acid properties during cladogenesis, and performs goodness-of-fit and categorical statistical tests based on ancestral sequence reconstruction. Amino-acid variability was estimated using the Selecton (Doron-Faigenboim et al. 2005; Stern et al. 2007) web server.

Test for Recombination

Recombination can confound phylogenetic and evolutionary selection analyses (Posada and Crandall 2002). Hence, we evaluated the effect of recombination on natriuretic and helokinestatin domains by employing Single Breakpoint Recombination and Genetic Algorithms for Recombination Detection (GARD) implemented in the Datamonkey server (Pond et al. 2005c, 2006; Delpont et al. 2010). Potential breakpoints were detected using the small sample Akaike Information Criterion (AIC) and the sequences were compartmentalized before conducting the aforementioned analyses.

Results

Histology

The mandibular toxin-secreting gland of *A. graminea* consists of numerous discrete compartments. Similar to those of other anguid lizards examined to-date (Fry et al. 2010b), there is an arrangement of one compartment per tooth (Fig. 1a). These glandular structures are enclosed by basally nucleated secretory epithelial cells that form a large vesicular region along the medial surface of the gland (Fig. 1b). The toxin vesicles appear to be released via exocytosis into the lumen of the toxin-secreting gland (Fig. 1b).

Toxin Molecular Evolution

BLAST analyses of transcripts recovered from *A. graminea* toxin-secreting gland cDNA libraries identified seven previously characterized toxiciferan toxins: CRiSP, cystatin, kallikrein, lectin, B-type natriuretic peptide, nerve growth factor, type III phospholipase A₂ and vascular endothelial growth factor. Phylogenetic analysis showed that they

clustered together with homologous sequences from the mandibular toxin-secreting gland of other anguimorph lizards and also homologous sequences produced by the maxillary venom glands of snakes. The VEGF sequences were an exception, forming a clade with snake similar snake venom gland forms not secreted into the venom rather than with the derived form secreted in snake venoms (Fig. 2).

Key functional residues were conserved for CRiSP and cystatin sequences and CRiSP sequences also conserved the cysteine pattern. The *A. graminea* lectin sequences contain the EPN tripeptide motif that facilitates hemotoxic activity via the mannose-binding site (Drickamer 1992; Fry et al. 2008, 2010b). Phylogenetically the *A. graminea* lectin sequences grouped with the sequence from *Varanus indicus* (which also contains the EPN motif), rather than with the sequence from the more closely related *Pseudopus [Ophisaurus] apodus* (which contains instead the galactose-binding QPD motif) (Fig. 3). We recovered the first full-length anguimorph lizard PLA₂ sequence obtained to-date and this was revealed to have an extraordinarily long pro-peptide domain within the precursor region (Fig. 4). The *A. graminea* PLA₂ also had a long C-terminal tail containing multiple di-basic post-translational cleavage sites previously noted as a characteristic of Anguimorpha lizard PLA₂ (Fry et al. 2006, 2009b, 2010b).

We also recovered kunitz peptides for the first time from any lizard oral secretion—this toxin had previously only been recorded from snake venoms. The fragment recovered was of the two-domain type only sequenced once from a snake (*Austrelaps labialis*) (Doley et al. 2008). For comparison's sake, we also sequenced a fragment from the mandibular venom gland of *Heloderma suspectum cinctum* and both anguimorph lizards contained the c-terminal extension (Fig. 5). Phylogenetic analysis recovered the lizard and *A. labialis* two-domain forms as basally divergent from all the mono-domain forms sequenced from snake venoms, and the snake venom forms were non-monophyletic (Fig. 6).

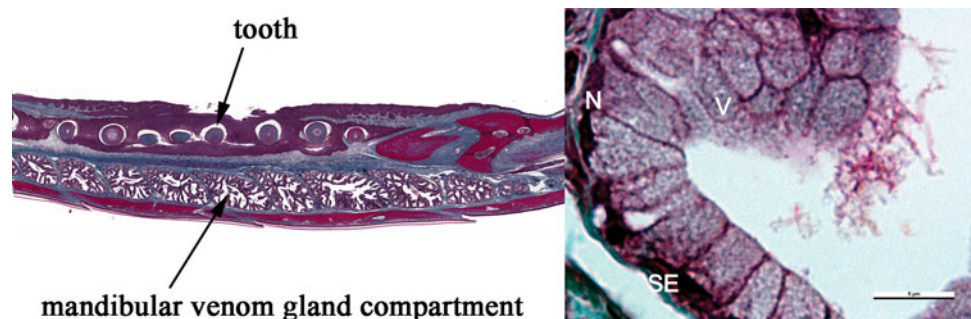


Fig. 1 **a** Masson's trichrome-stained transverse histology section of *A. graminea* showing the mixed seromucous lobules. Connective tissues surround individual regions or capsules of the toxin-secreting glands. **b** 100× view showing that these glandular structures consist

of secretory epithelium (SE) with basally nucleated (N) cells that are rich in enlarged vesicles (V) throughout their apical regions. Scale Bar = 5 μm

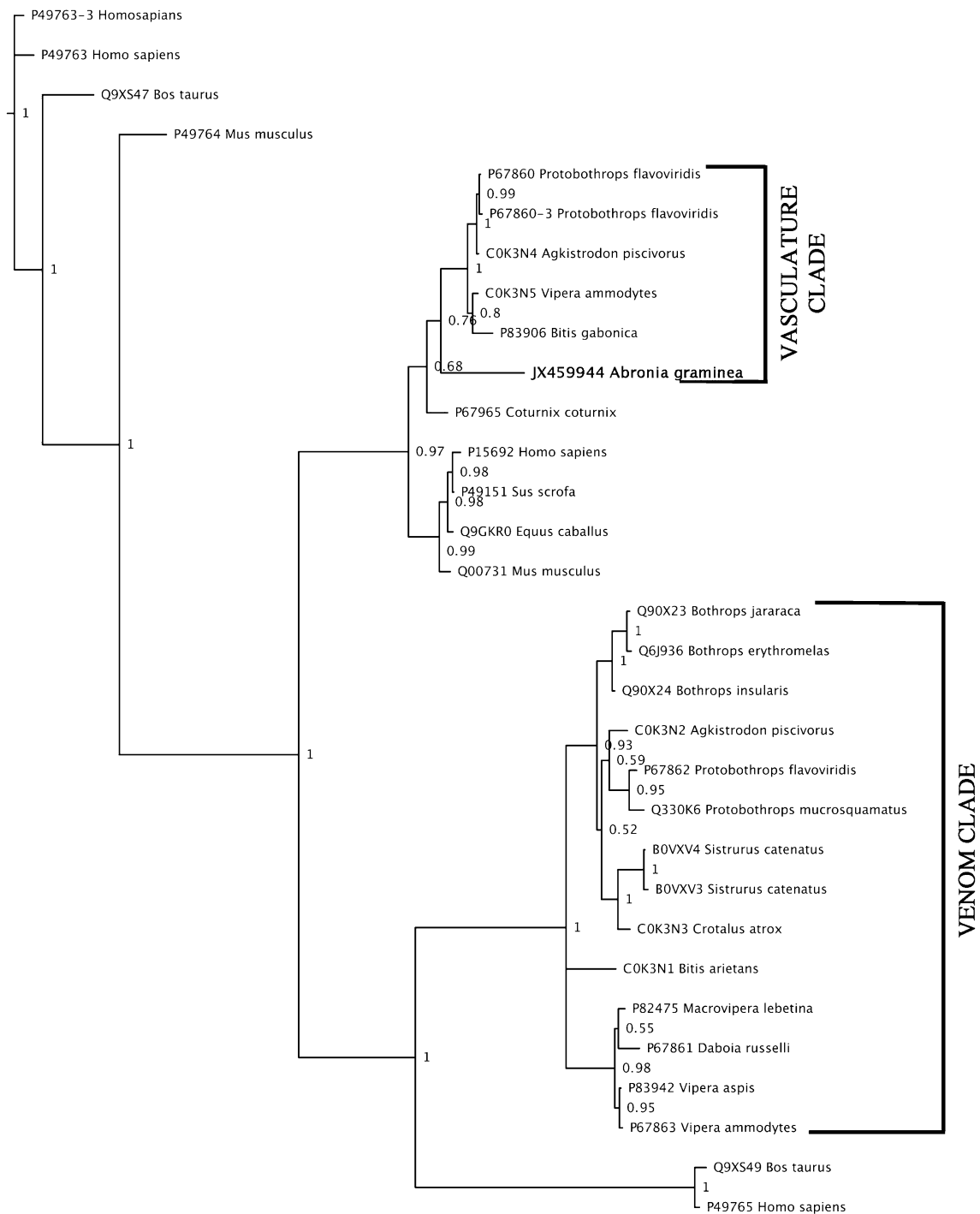


Fig. 2 Molecular phylogeny of VEGF. Outgroups are the non-toxin sequences from *Anser anser* (P83300) and *Rhea americana* (P84617)

The highest degree of molecular evolution was displayed in the natriuretic transcripts. All *A. graminea* natriuretic sequences share a pattern along with those from *G. infernalis* of five helokinestatin variants contained with the precursor region (Fig. 7). The *A. graminea* sequences also contain a new variant PPPFIPFIP inserted after the third shared

domain. This repeat preserves the conserved helokinestatin pattern of PPPxxPxxP, where the x residues are almost invariably hydrophobic (F, I, V, L). The domain encoding the natriuretic peptide shows the same high level of conservation shared with other anguimorph venom forms of this peptide. However, the *A. graminea* natriuretic peptide sequences

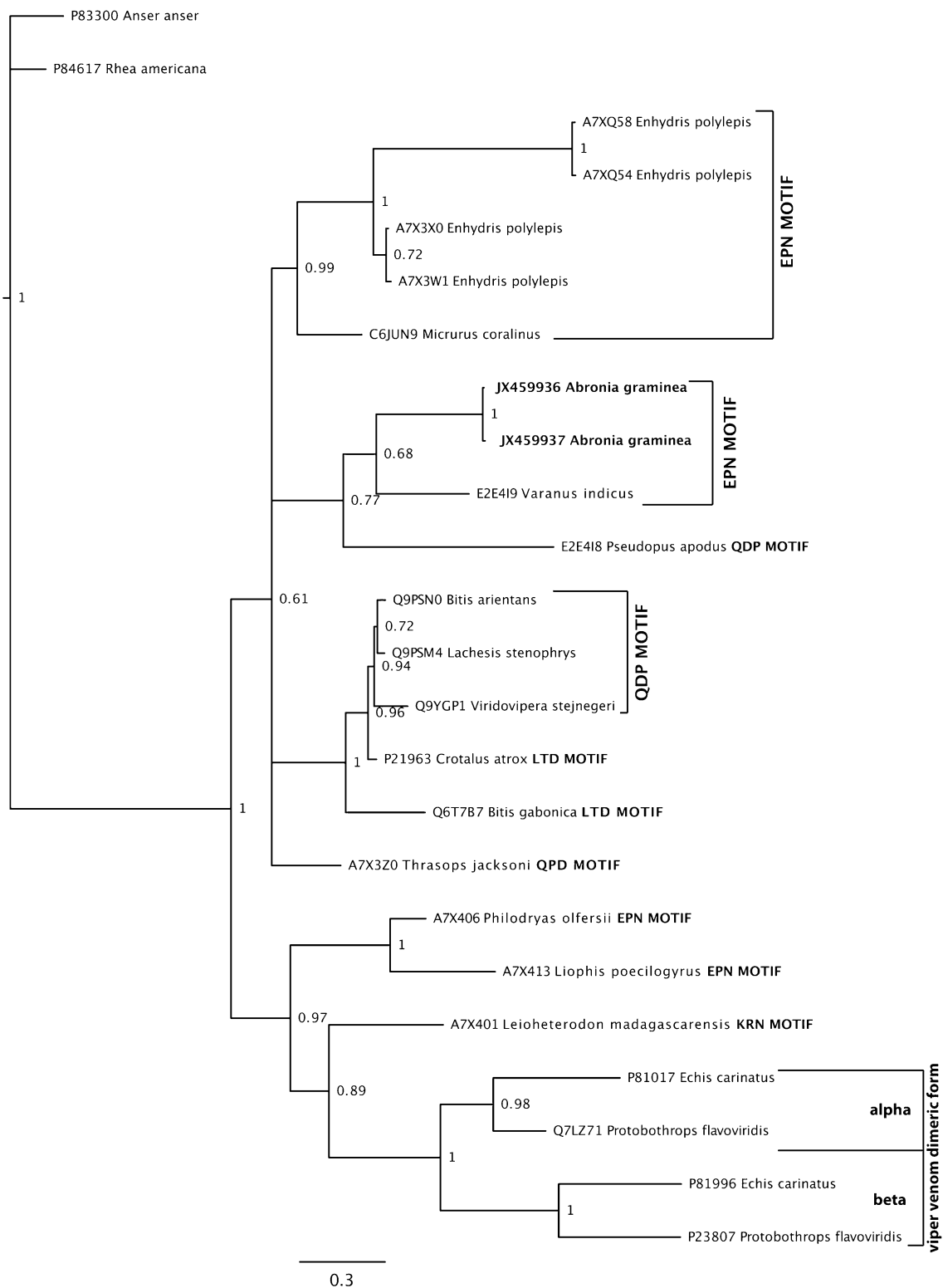


Fig. 3 Molecular phylogeny of lizard and snake lectin toxins. Outgroups are the non-toxin sequences from *Anser anser* (P83300) and *Rhea americana* (P84617)

share with those of *Gerrhonotus* the change to glutamic acid (E) from the ancestral key functional residue aspartic acid (D) at ring position 7. This is one of two mutations previously

shown by us to greatly reduce the aortic smooth muscle relaxing potency of the *Gerrhonotus* form (Fry et al. 2010b). The *A. graminea* sequences also uniquely contained the

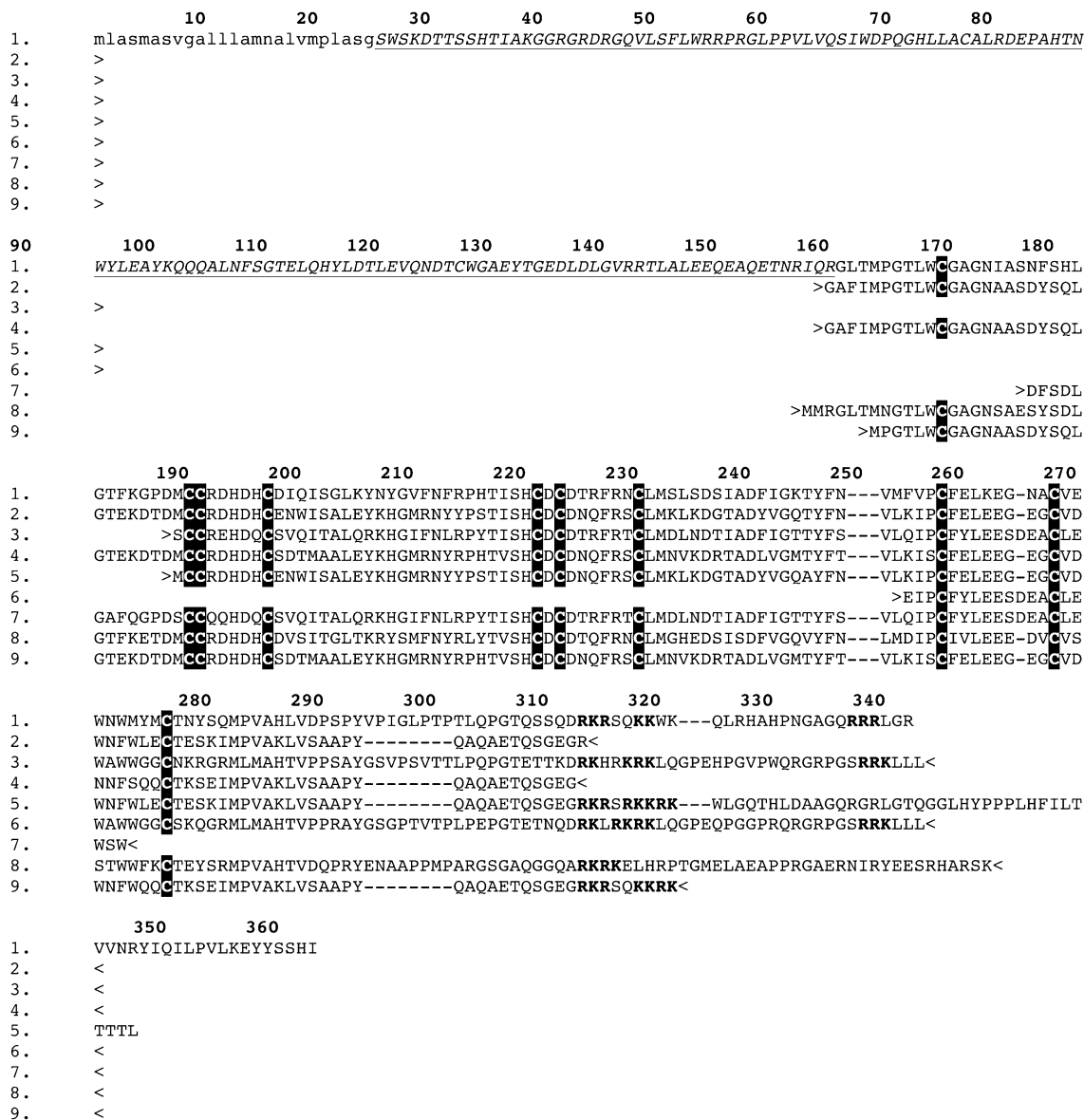


Fig. 4 Sequence alignment of lizard Type III phospholipase A toxins *I.A. graminea* (c9); 2. *Heloderma suspectum* (P16354); 3. *Varanus komodoensis* (B6CJU9); 4. *Heloderma suspectum* (P80003); 5. *Heloderma suspectum* (C6EVH0); 6. *Varanus gilleni* (E2E4K7);

7. *Varanus varius* (Q2XXL5); 8. *C. warreni* (E2E4K8) and 9. *Heloderma suspectum* (C6EVG9). Dibasic cleavage sites in bold and pro-pep is underlined

helokinestatin variant PPPFLPLVPR inserted after the fifth helokinestatin repeat.

The assumption of a single phylogenetic history for all sites in a sequence, which is a prerequisite for most phylogenetic analyses, can be violated by recombination which may cause elements with different genetic backgrounds to blend together. Thus, recombinant genes cannot be accurately described by a single/unique tree topology and recombination can influence selection analyses significantly by elevating false positives. Recombination can have more impact on the site-to-site and branch-to-branch omega estimations relative to the global estimates. We screened

natriuretic peptide and helokinestatin domains for recombination using GARD and SBP algorithms. GARD failed to identify any regions that underwent significant recombination. SPB however, identified a single potential breakpoint at the 100th position with a model-averaged support of 100 % and an IC (model with two trees) improvement of 79.73 over the base (single tree) model when using the AIC. Subsequent analyses were conducted by compartmentalizing the multiple sequence alignment into two non-recombinant units.

Initial selection analyses of full-length helokinestatin/natriuretic precursor (site-models, branch-models, branch-site models, SLAC, FEL, REL and evolutionary

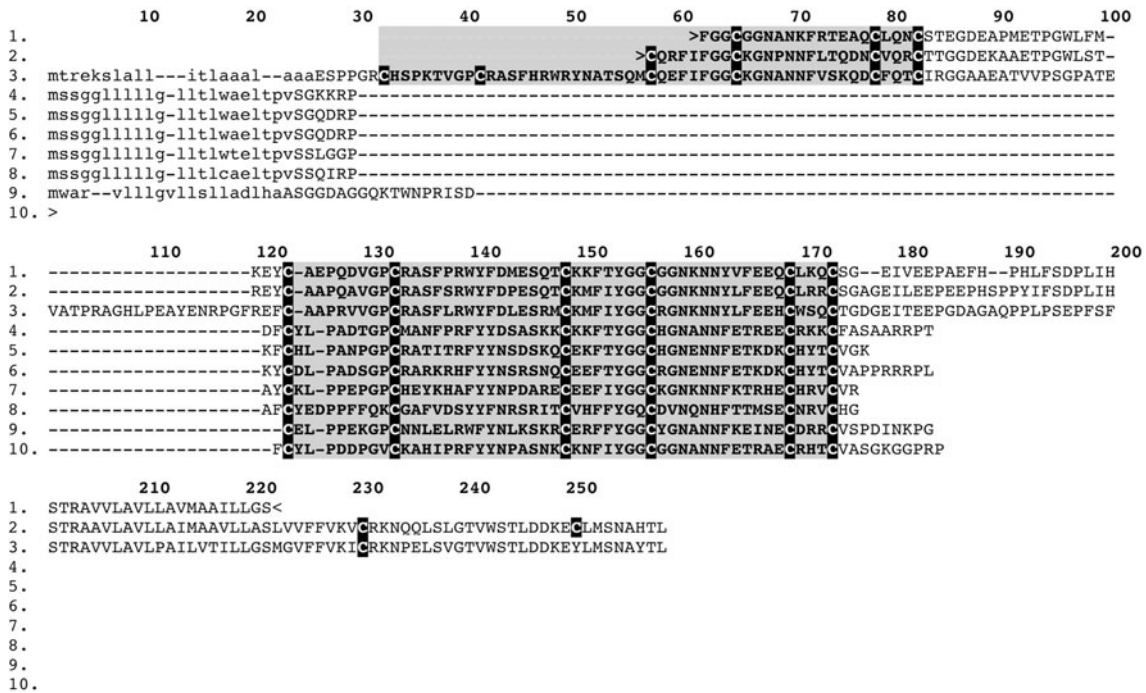


Fig. 5 Sequence alignment of kunitz peptides 1. *A. graminea*; 2. *Heloderma suspectum*; 3. B2BS84| *A. labialis*; 4. Q6T6S5 *Bitis gabonica*; 5. B5L5M7 *Austrelaps superbus*; 6. A7X3V4 *Telescopus*

dhara; 7. B2KTG1 *Bungarus fasciatus*; 8. G9I929 *Micrurus tener*; 9. A7X3V7 *Philodryas olfersii*; 10. P24541| *Eristicophis macmahoni*

fingerprinting) unanimously confirmed the high degree of conservation, a trend observed in the natriuretic domain of this proprotein in other anguimorph venoms investigated to-date (Tables 2, 3; Fig. 8) (Fry et al. 2006, 2009b, 2010a, b). This was confirmed by selection analyses at the level of the proteome conducted using TreeSAAP which apparently confirmed that none of the 31 biochemical or structural properties of this proprotein were under significant influence of selection.

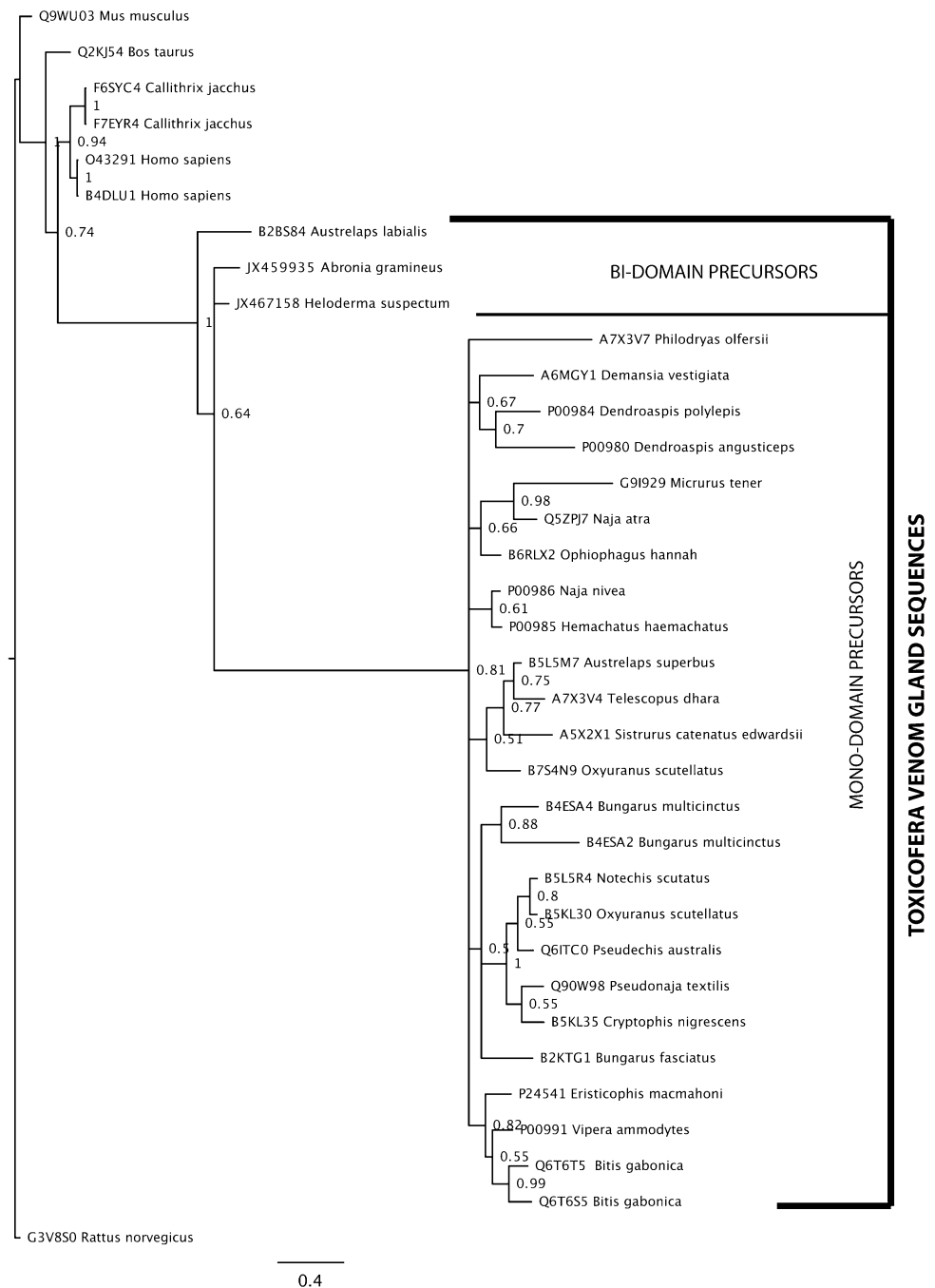
Although the branch and branch-site models failed to detect any significant positive selection, the free-ratio model, GA-branch and Branch-site REL tests identified a small proportion of sites within the *A. graminea* and *Heloderma* lineages that had undergone significant diversifying selection. In contrast, most of the varanid lizard natriuretic sequences appear to have evolved under negative selection. The observed diversifying selection in the *Abronia* and *Heloderma* sequences is a result of the presence of helokinestatin regions within them, which is unique to this clade and absent entirely in the varanid lizard venom form (Fry et al. 2006, 2009b, 2010a, b).

The two-speed rate of evolution was subsequently confirmed by compartmentalizing the sequences into helokinestatin and natriuretic domains and performing selection analyses in CODEML which revealed that the former exhibits weaker evolutionary constraints than the latter

($\omega = 0.60$ and 0.30 , respectively). Furthermore, investigations identified sites under the influence of positive Darwinian selection in the helokinestatin domain, in comparison with the natriuretic domain that largely remains under negative selection (Table 3). All the positively selected sites in the helokinestatin/natriuretic precursor detected by SLAC, FEL and REL came only from those that specifically encode the helokinestatin domain. On the other hand, 27 % of the sites in natriuretic peptides were under negative selection in comparison with the 5 % of the total residues of the helokinestatin domain. Out of the four codons detected by MEME test as under the influence of episodic diversifying selection (significance 0.05), three belonged to the helokinestatin domain whilst only one belonged to the natriuretic domain, further providing evidence for the differential selection pressures acting on the two domains of the proprotein (Table 3). Assignment of sites into variable and invariable categories using the selecton web server revealed a greater number of variable codons in the helokinestatin domain than the natriuretic domain (21.36 and 12.19 % of total codons, respectively). In addition, the helokinestatin domain contained fewer sites evolving under constrained selection pressures than the natriuretic domain (27.27 and 41.46 % of total codons, respectively—Table 3).

It should be noted that some varanid lizard lineages, namely *Varanus komodoensis* and one of the hypothetical

Fig. 6 Molecular phylogeny of lizard and snake kunitz toxins and related non-toxin sequences



ancestral clades (node 15: Fig. 8b and node 14: Fig. 8c), also exhibit a small proportion of sites with significant diversifying selection. This indicates that the positive evolutionary selection pressures act on the natriuretic peptide domain, a phenomenon previously observed in other toxiciferan venom components (Fry et al. 2006, 2009b, 2010a, b; Sunagar et al. 2012) and presumed to be the result of predator–prey co-evolutionary arms races. This could also be indicative of an active role for these components in the venom arsenal of these species.

Discussion

A ‘use it or lose it’ evolutionary trajectory has been documented previously in toxiciferan reptiles. Secondary loss or reduction of the venom system has been documented in several lineages of snakes including within highly toxic elapid clades (Li et al. 2005a, b; Fry et al. 2008, 2009a, b, Fry et al. 2010b, 2012). Thus, the presence of robust glands and evidence of active molecular evolution of some of the encoded proteins suggests that the toxin-secreting system is

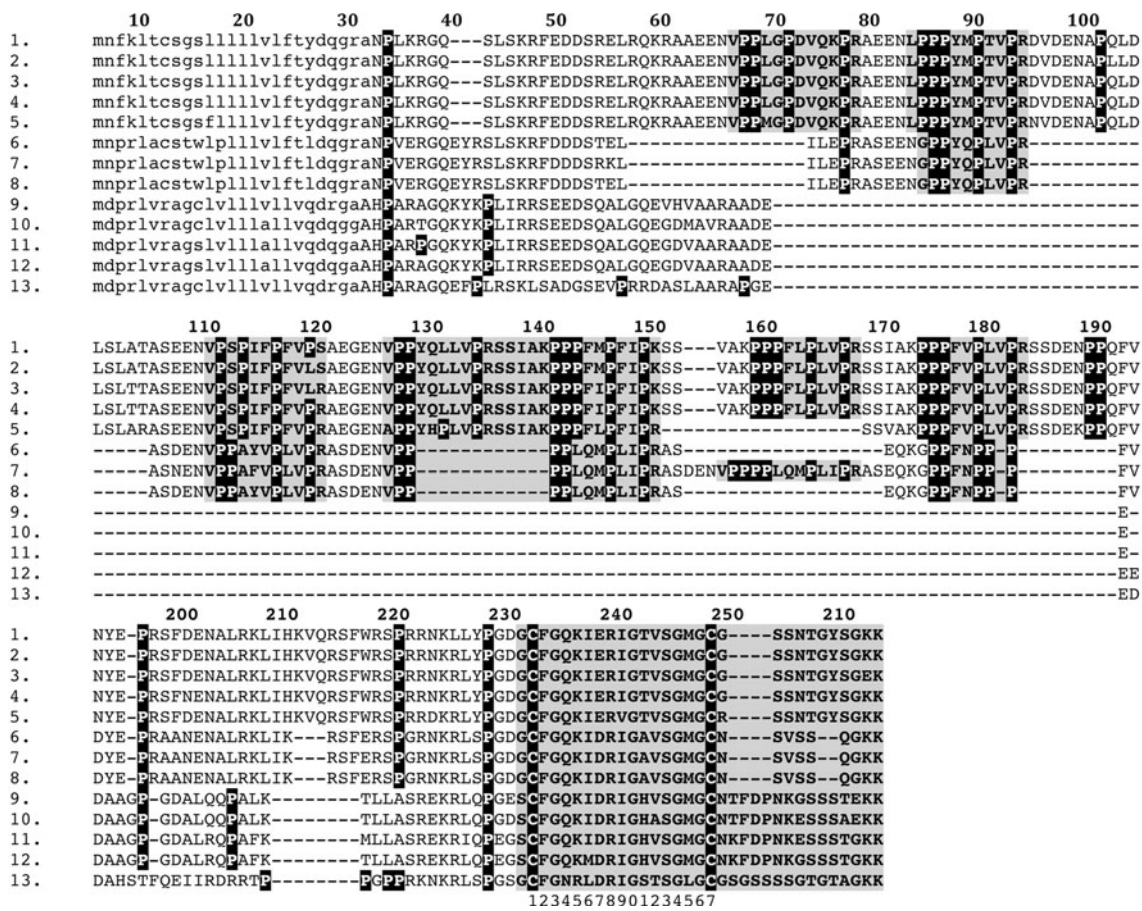


Fig. 7 Sequence alignment of lizard B-type natriuretic peptide toxins. 1. *A. graminea* (c648); 2. *A. graminea* (c448); 3. *A. graminea* (c731); 4. *A. graminea* (c776); 5. *G. infernalis* (E2E4J3); 6. *Heloderma suspectum* (C6EVG7); 7. *Heloderma horridum* (E8ZCG5); 8. *Heloderma suspectum* (D7FB57); 9. *Varanus glauerti*

(E2E4J0); 10. *Varanus scalaris* (E2E4J1); 11. *Varanus komodoensis* (B6CJV0); 12. *Varanus varius* (Q2XXL8); and 13. *Varanus glauerti* (E2E4J2). Helokinestatin domains are highlighted in light grey, natriuretic domains in dark grey

biologically and ecologically relevant for *A. graminea*. The *A. graminea* toxin-secreting glands examined in this study exhibited signs of active secretion, with cells full of secretory granules. In addition, the molecular evolution of *A. graminea* toxins displayed varying rates of evolution between different protein types, which provides further evidence that these components are biologically relevant and are ‘seen’ by active selection pressures. Some molecular derivations appear lineage-specific. For example addition to the ancestral kallikrein cysteine arrangement, a form was found in the *A. graminea* library that has only ever been recovered from the mandibular toxin-secreting glands other anguillid lizards (*C. warreni* and *G. infernalis*—(Fry et al. 2010b)). (This anguillid-specific isoform includes a deletion resulting in the loss of 12th ancestral cysteine and the insertion of a new cysteine in between ancestral cysteines 9 and 10. We also showed for the first time that the kunitz peptide toxin type is ancestral to all toxiciferan reptiles, as evidenced by the snake sequences being non-monophyletic relative to the lizard sequences.

The helokinestatin encoding domain which has evolved de novo within the natriuretic precursor pro-pep region displayed the most active molecular evolution of any toxin transcript recovered in this study. Several sequences of this toxin type possessed sites undergoing significant episodic diversifying selection, which may be indicative of the active role of this component in the toxic arsenal of *A. graminea*. Thus, it would be quite interesting for future studies to assess the effect of the presence/absence of helokinestatin on the pharmacological activity of the oral secretions. In contrast, the natriuretic peptide encoding domain located just downstream of this element exhibits tremendous conservation. This shows that even very closely related toxins can undergo differential selection pressures. The natriuretic peptide region highlights the usefulness of toxins in understanding the structure–function relationships of the ancestral body form. We previously showed that the change from D (glutamic acid) to E (aspartic acid) at ring position 7 and I (isoleucine) to V (valine) at ring position 9 both resulted in significant

Table 2 Maximum-likelihood parameter estimates for the helokinestatin and natriuretic peptides

Model	Likelihood (l)	ω_0^a	Parameters	Sign. ^b	No. of Sites with $\omega > 1^c$ B.E.B
M0 (one ratio)	-1456.052653	0.38	$=\omega_0$		-
M1 (neutral)	-1441.300937	0.45	$P_0: 0.666$ $\omega_0: 0.18$ $P_1: 0.333$ $\omega_1: 1.0$	$P < 0.05$	-
M2 (selection)*	-1440.921863	0.51	$P_0: 0.701$ $\omega_0: 0.21$ $P_1: 0.218$ $\omega_1: 1.0$ $P_2: 0.079$ $\omega_2: 1.84$		0 (PP ≥ 0.99) 0 (P ≥ 0.95)
M3 (discrete)*	-1440.606756	0.51	$P_0: 0.354$ $\omega_1: 0.11$ $P_1: 0.478$ $\omega_1: 0.41$ $P_2: 0.166$ $\omega_2: 1.65$	$P \ll 0.001$	-
M7 (beta)	-1443.054501	0.42	$p: 0.70303$ $q: 0.93123$	$P < 0.05$	-
M8 (beta and ω)*	-1440.630830	0.51	$p_0: 0.838$ $p: 1.811$ $q: 4.298$ $p_1: 0.161$ $\omega: 1.66$		0 (PP ≥ 0.99) 0 (P ≥ 0.95)

* Models which allow $\omega > 1$

^a dn/ds (weighted average)

^b Significance of the model in comparison with the null model

^c Number of sites with $\omega > 1$ under the BEB approach with a posterior probability (PP) more than or equal to 0.99 and 0.95

Table 3 Comparison of natriuretic and helokinestatin domain evolution

	SLAC ^a	FEL ^b	REL ^c	Integrative analyses SLAC + FEL + REL + MEME	MEME ^d	Selecton ^e	Domain comparison Codeml (option G, mgene = 4)
Helokinestatin domain	$\omega > 1^f$	0	2	0	3		$\omega = 0.600$
	$\omega < 1^g$	1	10	1	11	3	47 (21.36 %) 60 (27.27 %)
Natriuretic domain	$\omega > 1^f$	0	0	0	0		$\omega = 0.304$
	$\omega < 1^g$	1	9	8	12	1	5 (12.19 %) 17 (41.46 %)

ω Mean dN/dS

^a Single likelihood ancestor counting

^b Fixed-effects likelihood

^c Random-effects likelihood

^d Sites detected as experiencing episodic diversifying selection (0.05 significance) by the Mixed Effects Model Evolution (MEME)

^e Number of positively and negatively selected sites detected by the selecton server

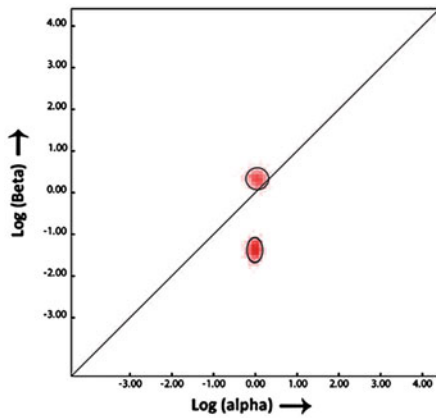
^f Number of positively selected sites at 0.05 significance (for SLAC, FEL) or 50 Bayes factor (for REL)

^g Number of negatively selected sites at 0.05 significance (for SLAC, FEL) or 50 Bayes factor (for REL)

reduction in the potency of action upon vascular smooth muscle (Fry et al. 2010b). Both changes would normally be considered as conserved substitutions as they are negative/negative and hydrophobic/hydrophobic, respectively. In both cases however, whilst the substitutions have

essentially the same chemical properties, they result in steric differences. This mirrors and reinforces the exquisite subtlety of venom peptide targeting. The extraordinarily long pro-pep region of the *A. graminea* PLA₂ may ultimately be shown to contain also post-translationally

A Evolutionary Fingerprint

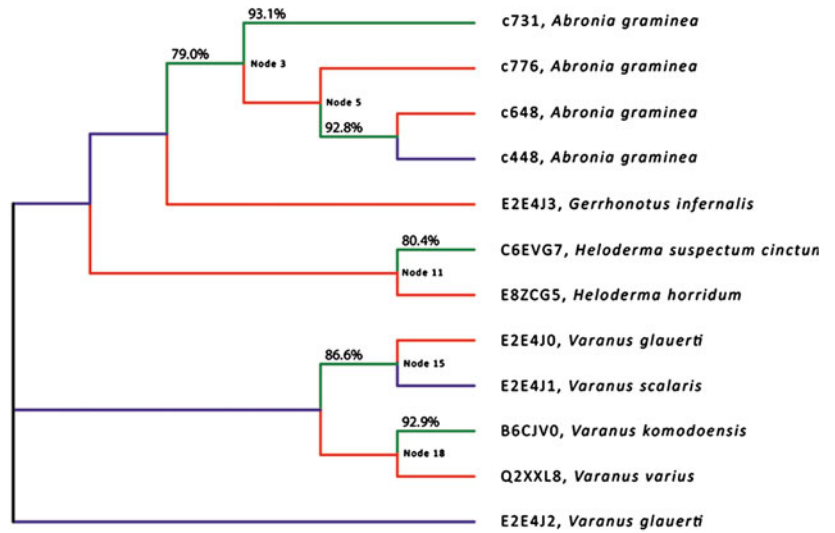


Omega (ω) = 0.51
(Site Model M8)

SLAC, FEL, REL, MEME
(Integrative)

Positively Selected: 4
Negatively Selected: 23

B GA-Branch Test

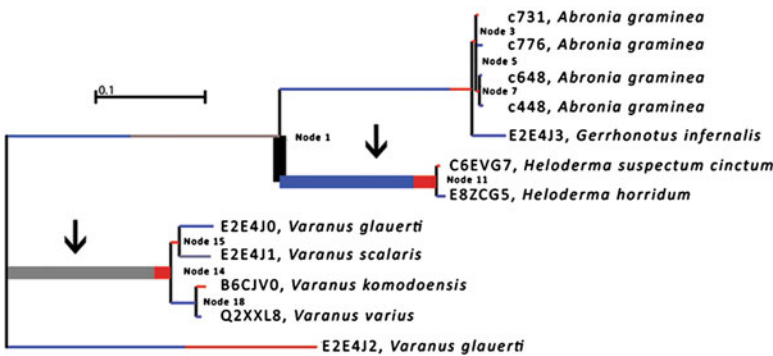


■ **Omega (ω) = 0.291** (21% of sites)

■ **Omega (ω) = 0.631** (76% of sites)

■ **Omega (ω) = 10,000** (3% of sites)

C Branch-site REL



■ **Omega (ω) > 5, Episodic Diversifying Selection**

■ **Omega (ω) = 0, Negative Selection**

■ **Omega (ω) = 1, Neutral Selection**

Fig. 8 Evolutionary fingerprinting of natriuretic and helokinesstatin propeptide and the test for detection of sites under episodic diversifying selection. **a** Evolutionary fingerprint: Estimates of the distribution of synonymous (α) and non-synonymous (β) substitution rates inferred for natriuretic and helokinesstatin propeptide. The ellipses reflect a Gaussian-approximated variance in each individual rate estimate, and coloured pixels show the density of the posterior sample of the distribution for a given rate. The *diagonal line* represents the idealized neutral evolution regime ($\omega = 1$), points above and below the *line* correspond to positive selection ($\omega > 1$) and negative selection ($\omega < 1$), respectively. The legend label shows the omega estimation under the site model M8 (Codeml) and the number of positive and

negatively selected residues detected by the integrative analyses (SLAC, FEL, REL and MEME). **b** GA-branch test: Lineages under different regimes of selection pressures are coloured differently and the accuracy with which they can be ascribed to that regime is denoted above them. The legend labels show the total percentage of the tree with respective dN/dS. **c** Branch-site REL: The strengths of different selection pressures, namely, positive, negative and neutral are indicated by different hues (*red*, *blue* and *grey*, respectively) with the width of each colour component indicating the proportion of sites in the corresponding class. Branches detected as undergoing episodic diversifying selection by the sequential LRTs at corrected $P \leq 0.05$ are denoted by *arrows* (Color figure online)

liberated peptides, as has been demonstrated for some of the other precursors with lengthy pro-pep regions such as the helokinstatin/natriuretic precursors.

The NGF and VEGF sequences were interesting in their relationships to non-toxin sequences. The NGF sequences also seem to be under profound evolutionary constraints. Intriguingly, the *A. graminea* and snake venom gland transcripts of this protein are virtually identical to the *G. infernalis* (E2E4J3) and *Heloderma suspectum* (C6EVG7) nuclear gene sequences obtained for use in taxonomical studies (Wiens et al. 2010). This indicates that the NGF expressed in venom may be the same gene as is used in the body and therefore may be a rare case of a venom protein resulting from a non-duplicated gene. The VEGF sequences reinforce the value of phylogenetic analyses to establish homology, as there are two clades of VEGF that have been sequenced from snake venom glands: one type that is a part of the vasculature of the venom gland and the other type which is the form actually secreted in the venom. The form recovered in this study was of the former type and thus the VEGF toxins are not known to-date as a basal toxiciferan venom component and appear to be restricted to the advanced snakes. Consistent with the distinction between the body form of a protein and its toxin homologue, the vascular VEGF display much less sequence variation than the venom sequences, indicating that they are evolving under negative selection whilst the actively secreted forms are evolving under positive selection.

Our results show that even small arboreal anguimorpha lizard lineages retain the ancestral venom system and that the continued diversification is indicative of continued evolution operating under selection pressure. Thus, these lizards are technically venomous. It should be stressed, however, that in no way do we suggest that these animals are 'venomous' from the perspective of a threat to human health and thus should not be considered as 'venomous' from the stand-point of dangerous animal legislation. We instead consider the analogy with spiders to be relevant: like spiders, anguimorpha lizards are venomous from a biological/evolutionary perspective but are harmless from the perspective of human health.

Due to the relative sampling employed, the toxin types recovered in this study from the mandibular venom gland of *A. graminea* are no doubt but a subset of the total diversity encoded. More intensive sampling would almost certainly recover novel isoforms of known toxin types, perhaps even changing our knowledge of the timing of recruitment events, as well as even recovering entirely new suites of bioactive compounds. Regardless, this study has advanced our knowledge of lizard venom evolution by showing that even obscure arboreal species can be a rich source of novel sequences. Such new information is not only just of use for evolutionary investigations but also

provides a pragmatic platform for the investigation of novel components as lead compounds in drug design and development. The strong evidence of positive selection on certain secretory toxins as well as the evolutionary conservation of others is highly suggestive of the active use of these secretory toxins in the ecology (either predatory or defensive) of this anguimorph lizard. Confirmation in future studies of the presence of these toxins in the secretory-proteome of *A. graminea* will add further strength to the hypothesis that the toxin-secreting oral glands of many toxiciferan lizards are not merely examples of 'exaptation' (for future development into 'true venom glands') but play an important role in the ecology of these species and are thus true 'venom glands' by any definition.

Acknowledgments BGF was funded by the Australian Research Council and the University of Queensland. EABU would like to acknowledge funding from the University of Queensland (International Postgraduate Research Scholarship, UQ Centennial Scholarship, and UQ Advantage Top-Up Scholarship) and the Norwegian State Education Loans Fund. This research was supported in part by the Portuguese Foundation for Science and Technology (FCT) through the Ph.D. grant conferred to KS (SFRH/BD/61959/2009) and the project PTDC/AAC-AMB/121301/2010 (FCOMP-01-0124-FEDER-019490) to AA.

Conflict of interest None.

References

- Altschul SF, Madden TL, Schaffer AA, Zhang JH, Zhang Z, Miller W, Lipman DJ (1997) Gapped BLAST and PSI-BLAST: a new generation of protein database search programs. *Nucleic Acids Res* 25:3389–3402
- Anisimova M, Bielawski JP, Yang ZH (2002) Accuracy and power of Bayes prediction of amino acid sites under positive selection. *Mol Biol Evol* 19:950–958
- Beck DD (2005) Biology of gila monsters and beaded lizards. University of California Press, Berkeley
- Bogert CM, del Campo RM (1956) The gila monster and its allies. The relationships, habits, and behavior of the lizards of the family Helodermatidae. *Bull Am Mus Nat Hist* 109:1–238
- Bouaboud CF, Kardassakis DG (1988) Acute myocardial-infarction following a gila monster (*Heloderma suspectum cinctum*) bite. *West J Med* 148:577–579
- Cantrell FL (2003) Envenomation by the Mexican beaded lizard: a case report. *J Toxicol Clin Toxicol* 41:241–244
- Casewell NR, Huttley GA, Wuester W (2012) Dynamic evolution of venom proteins in squamate reptiles. *Nat Commun* 3:1066. doi: [10.1038/ncomms2065](https://doi.org/10.1038/ncomms2065)
- Clemetson KJ, Lu QM, Clemetson JM (2005) Snake C-type lectin-like proteins and platelet receptors. *Pathophysiol Haemost Thromb* 34:150–155
- Conesa A, Gotz S (2008) Blast2GO: a comprehensive suite for functional analysis in plant genomics. *Int J Plant Genomics* 2008:619832
- Conesa A, Gotz S, Garcia-Gomez JM, Terol J, Talon M, Robles M (2005) Blast2GO: a universal tool for annotation, visualization and analysis in functional genomics research. *Bioinformatics* 21:3674–3676

- Datta G, Tu AT (1997) Structure and other chemical characterizations of gila toxin, a lethal toxin from lizard venom. *J Pept Res* 50: 443–450
- Delport W, Poon AFY, Frost SDW, Pond SLK (2010) Datamonkey 2010: a suite of phylogenetic analysis tools for evolutionary biology. *Bioinformatics* 26:2455–2457
- Doley R, Nguyen NBT, Reza MA, Kini RM (2008) Unusual accelerated rate of deletions and insertions in toxin genes in the venom glands of the pygmy copperhead (*Austrelaps labialis*) from Kangaroo island. *BMC Evol Biol* 8:1–13
- Doron-Faigenboim A, Stern A, Bacharach E, Pupko T (2005) Selecton: a server for detecting evolutionary forces at a single amino-acid site. *Bioinformatics* 21:2101–2103
- Drickamer K (1992) Engineering galactose-binding activity into a c-type mannose-binding protein. *Nature* 360:183–186
- Fry BG, Wickramaratana JC, Lemme S, Beuve A, Garbers D, Hodgson WC, Alewood P (2005) Novel natriuretic peptides from the venom of the inland taipan (*Oxyuranus microlepidotus*): isolation, chemical and biological characterisation. *Biochem Biophys Res Commun* 327:1011–1015
- Fry BG, Vidal N, Norman JA, Vonk FJ, Scheib H, Ramjan SF, Kuruppu S, Fung K, Hedges SB, Richardson MK, Hodgson WC, Ignjatovic V, Summerhayes R, Kochva E (2006) Early evolution of the venom system in lizards and snakes. *Nature* 439:584–588
- Fry BG, Scheib H, van der Weerd L, Young B, McNaughtan J, Ramjan SF, Vidal N, Poelmann RE, Norman JA (2008) Evolution of an arsenal: structural and functional diversification of the venom system in the advanced snakes (Caenophidia). *Mol Cell Proteomics* 7:215–246
- Fry BG, Vidal N, van der Weerd L, Kochva E, Renjifo C (2009a) Evolution and diversification of the Toxicofera reptile venom system. *J Proteomics* 72:127–136
- Fry BG, Wroe S, Teeuwisse W, van Osch MJ, Moreno K, Ingle J, McHenry C, Ferrara T, Clausen P, Scheib H, Winter KL, Griesman L, Roelants K, van der Weerd L, Clemente CJ, Giannakis E, Hodgson WC, Luz S, Martelli P, Krishnasamy K, Kochva E, Kwok HF, Scanlon D, Karas J, Citron DM, Goldstein EJ, McNaughtan JE, Norman JA (2009b) A central role for venom in predation by *Varanus komodoensis* (Komodo Dragon) and the extinct giant *Varanus (Megalania) priscus*. *Proc Natl Acad Sci USA* 106:8969–8974
- Fry BG, Roelants K, Winter K, Hodgson WC, Griesman L, Kwok HF, Scanlon D, Karas J, Shaw C, Wong L, Norman JA (2010a) Novel venom proteins produced by differential domain-expression strategies in beaded lizards and gila monsters (genus *Heloderma*). *Mol Biol Evol* 27:395–407
- Fry BG, Winter K, Norman JA, Roelants K, Nabuurs RJ, van Osch MJ, Teeuwisse WM, van der Weerd L, McNaughtan JE, Kwok HF, Scheib H, Griesman L, Kochva E, Miller LJ, Gao F, Karas J, Scanlon D, Lin F, Kuruppu S, Shaw C, Wong L, Hodgson WC (2010b) Functional and structural diversification of the Anguimorpha lizard venom system. *Mol Cell Proteomics* 9:2369–2390
- Fry BG, Casewell NR, Wüster W, Vidal N, Young B, Jackson TNW (2012) The structural and functional diversification of the Toxicofera reptile venom system. *Toxicon* 9(11):2369–2390
- Goetz S, Arnold R, Sebastian-Leon P, Martin-Rodriguez S, Tischler P, Jehl M-A, Dopazo J, Rattei T, Conesa A (2011) B2G-FAR, a species-centered GO annotation repository. *Bioinformatics* 27:919–924
- Gotz S, Garcia-Gomez JM, Terol J, Williams TD, Nagaraj SH, Nueda MJ, Robles M, Talon M, Dopazo J, Conesa A (2008) High-throughput functional annotation and data mining with the Blast2GO suite. *Nucleic Acids Res* 36:3420–3435
- Hooker KR, Caravati EM (1994) Gila monster envenomation. *Ann Emerg Med* 24:731–735
- Huang TF, Chiang HS (1994) Effect on human platelet-aggregation of phospholipase a(2) purified from *Heloderma horridum* (beaded lizard) venom. *Biochim Biophys Acta* 1211:61–68
- Komori Y, Nikai T, Sugihara H (1988) Purification and characterization of a lethal toxin from the venom of *Heloderma horridum horridum*. *Biochem Biophys Res Commun* 154:613–619
- Kwok HF, Chen T, O'Rourke M, Ivanyi C, Hirst D, Shaw C (2008) Helokinstatin: a new bradykinin B-2 receptor antagonist decapeptide from lizard venom. *Peptides* 29:65–72
- Li M, Fry BG, Kini RM (2005a) Eggs-only diet: its implications for the toxin profile changes and ecology of the marbled sea snake (*Aipysurus eydouxii*). *J Mol Evol* 60:81–89
- Li M, Fry BG, Kini RM (2005b) Putting the brakes on snake venom evolution: the unique molecular evolutionary patterns of *Aipysurus eydouxii* (Marbled sea snake) phospholipase A(2) toxins. *Mol Biol Evol* 22:934–941
- Ma CB, Wang H, Wu YX, Zhou M, Lowe G, Wang L, Zhang YQ, Chen TB, Shaw C (2012) Helokinstatin-7 peptides from the venoms of *Heloderma* lizards. *Peptides* 35:300–305
- Mebis D (1969a) Isolation and properties of kallikrein from venom of gila monster (*Heloderma suspectum*). *Hoppe Seylers Z Physiol Chem* 350:821–826
- Mebis D (1969b) Purification and properties of a kinin liberating enzyme from venom of *Heloderma suspectum*. *Naunyn-Schmiedeberg Arch Pharmacol* 264:280–281
- Mochcamorales J, Martin BM, Possani LD (1990) Isolation and characterization of helothermine, a novel toxin from *Heloderma horridum horridum* (mexican beaded lizard) venom. *Toxicon* 28:299–309
- Morita T (2005) Structures and functions of snake venom CLPs (C-type lectin-like proteins) with anticoagulant-, procoagulant-, and platelet-modulating activities. *Toxicon* 45:1099–1114
- Morrisette J, Elhayek R, Possani L, Coronado R (1994) Isolation and characterization of ryanodine receptor toxins from *Heloderma horridum* (mexican beaded lizard) venom. *Biophys J* 66:A415
- Morrisette J, Kratzschmar J, Haendler B, Elhayek R, Mochcamorales J, Martin BM, Patel JR, Moss RL, Schleuning WD, Coronado R, Possani LD (1995) Primary structure and properties of helothermine, a peptide toxin that blocks ryanodine receptors. *Biophys J* 68:2280–2288
- Nielsen R, Yang ZH (1998) Likelihood models for detecting positively selected amino acid sites and applications to the HIV-1 envelope gene. *Genetics* 148:929–936
- Nikai T, Imai K, Sugihara H, Tu AT (1988) Isolation and characterization of horridum toxin with arginine ester hydrolase activity from *Heloderma horridum* (beaded lizard) venom. *Arch Biochem Biophys* 264:270–280
- Nikai T, Imai K, Komori Y, Sugihara H (1992) Isolation and characterization of arginine ester hydrolase from *Heloderma horridum* (beaded lizard) venom. *Int J Biochem* 24:415–420
- Nobile M, Magnelli V, Lagostena L, Mochcamorales J, Possani LD, Prestipino G (1994) The toxin helothermine affects potassium currents in newborn rat cerebellar granule cells. *J Membr Biol* 139:49–55
- Nobile M, Noceti F, Prestipino G, Possani LD (1996) Helothermine, a lizard venom toxin, inhibits calcium current in cerebellar granules. *Exp Brain Res* 110:15–20
- Piskurek O, Austin CC, Okada N (2006) Sauria SINES: novel short, interspersed retroposable elements that are widespread in reptile genomes. *J Mol Evol* 62:630–644
- Pond SLK, Frost SDW (2005a) Not so different after all: a comparison of methods for detecting amino acid sites under selection. *Mol Biol Evol* 22:1208–1222
- Pond SLK, Frost SDW (2005b) A genetic algorithm approach to detecting lineage-specific variation in selection pressure. *Mol Biol Evol* 22:478–485

- Pond SLK, Frost SDW, Muse SV (2005) HyPhy: hypothesis testing using phylogenies. *Bioinformatics* 21:676–679
- Pond SLK, Posada D, Gravenor MB, Woelk CH, Frost SDW (2006) Automated phylogenetic detection of recombination using a genetic algorithm. *Mol Biol Evol* 23:1891–1901
- Pond SLK, Murrell B, Fourment M, Frost SDW, Delport W, Scheffler K (2011) A random effects branch-site model for detecting episodic diversifying selection. *Mol Biol Evol* 28:3033–3043
- Posada D, Crandall KA (2002) The effect of recombination on the accuracy of phylogeny estimation. *J Mol Evol* 54:396–402
- Ronquist F, Huelsenbeck JP (2003) MrBayes 3: bayesian phylogenetic inference under mixed models. *Bioinformatics* 19:1572–1574
- Stern A, Doron-Faigenboim A, Erez E, Martz E, Bacharach E, Pupko T (2007) Selecton 2007: advanced models for detecting positive and purifying selection using a Bayesian inference approach. *Nucleic Acids Res* 35:W506–W511
- Strimble PD, Tomassoni AJ, Otten EJ, Bahner D (1997) Report on envenomation by a Gila monster (*Heloderma suspectum*) with a discussion of venom apparatus, clinical findings, and treatment. *Wilderness Environ Med* 8:111–116
- Sunagar K, Johnson WE, O'Brien SJ, Vasconcelos V, Antunes A (2012) Evolution of CRISPs associated with toxiciferan-reptilian venom and mammalian reproduction. *Mol Biol Evol* 29:1807–1822
- Suzuki Y, Nei M (2004) False-positive selection identified by ML-based methods: examples from the Sig1 gene of the diatom *Thalassiosira weissflogii* and the tax gene of a human T-cell lymphotropic virus. *Mol Biol Evol* 21:914–921
- Tu AT, Hendon RR (1983) Characterization of lizard venom hyaluronidase and evidence for its action as a spreading factor. *Comp Biochem Physiol B* 76:377–383
- Utainsincharoen P, Mackessy SP, Miller RA, Tu AT (1993) Complete primary structure and biochemical-properties of gilatoxin, a serine-protease with kallikrein-like and angiotensin-degrading activities. *J Biol Chem* 268:21975–21983
- Vidal N, Hedges SB (2005) The phylogeny of squamate reptiles (lizards, snakes, and amphisbaenians) inferred from nine nuclear protein-coding genes. *C R Biol* 328:1000–1008
- Wiens JJ, Kuczynski CA, Townsend T, Reeder TW, Mulcahy DG, Sites JW Jr (2010) Combining phylogenomics and fossils in higher-level squamate reptile phylogeny: molecular data change the placement of fossil taxa. *Syst Biol* 59:674–688
- Wiens JJ, Hutter CR, Mulcahy DG, Noonan BP, Townsend TM, Sites JW, Reeder TW (2012) Resolving the phylogeny of lizards, and snakes (squamata), with extensive sampling, of genes and species. *Biol Lett* 8(6):1043–1046
- Woolley S, Johnson J, Smith MJ, Crandall KA, McClellan DA (2003) TreeSAAP: selection on amino acid properties using phylogenetic trees. *Bioinformatics* 19:671–672
- Yang Z (2007) PAML 4: phylogenetic analysis by maximum likelihood. *Mol Biol Evol* 24:1586–1591
- Yang ZH, Nielsen R (2002) Codon-substitution models for detecting molecular adaptation at individual sites along specific lineages. *Mol Biol Evol* 19:908–917
- Yang ZH, Wong WSW, Nielsen R (2005) Bayes empirical Bayes inference of amino acid sites under positive selection. *Mol Biol Evol* 22:1107–1118
- Zhang JZ, Nielsen R, Yang ZH (2005) Evaluation of an improved branch-site likelihood method for detecting positive selection at the molecular level. *Mol Biol Evol* 22:2472–2479